

This pdf file consists of figures containing photographs, and their captions,  
scanned from:

MESOZOIC AND CENOZOIC THERMAL HISTORY OF THE EASTERN MOJAVE  
DESERT, CALIFORNIA AND WESTERN ARIZONA, WITH EMPHASIS ON THE  
OLD WOMAN MOUNTAINS AREA AND THE CHEMEHUEVI METAMORPHIC  
CORE COMPLEX

by

David A. Foster

A Dissertation

Submitted to the State University of New York at Albany

in Partial Fulfillment of

the Requirements for the Degree of

Doctor of Philosophy

College of Sciences and Mathematics

Department of Geological Sciences

1989

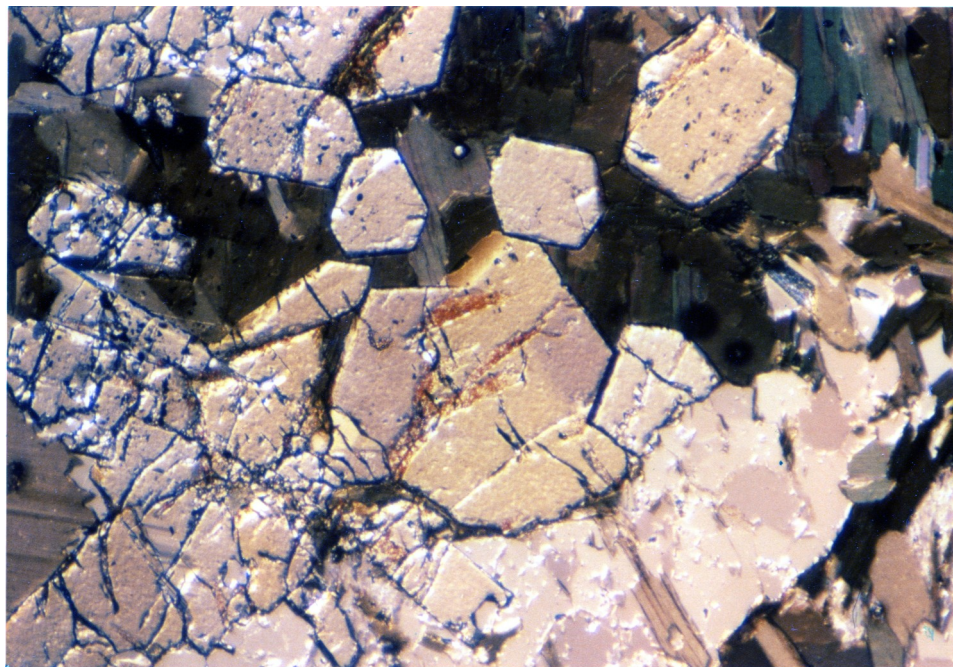


Figure 3-22. Photomicrograph of sample PM32b showing late porphyroblasts of biotite and staurolite (long direction is ~5 mm).

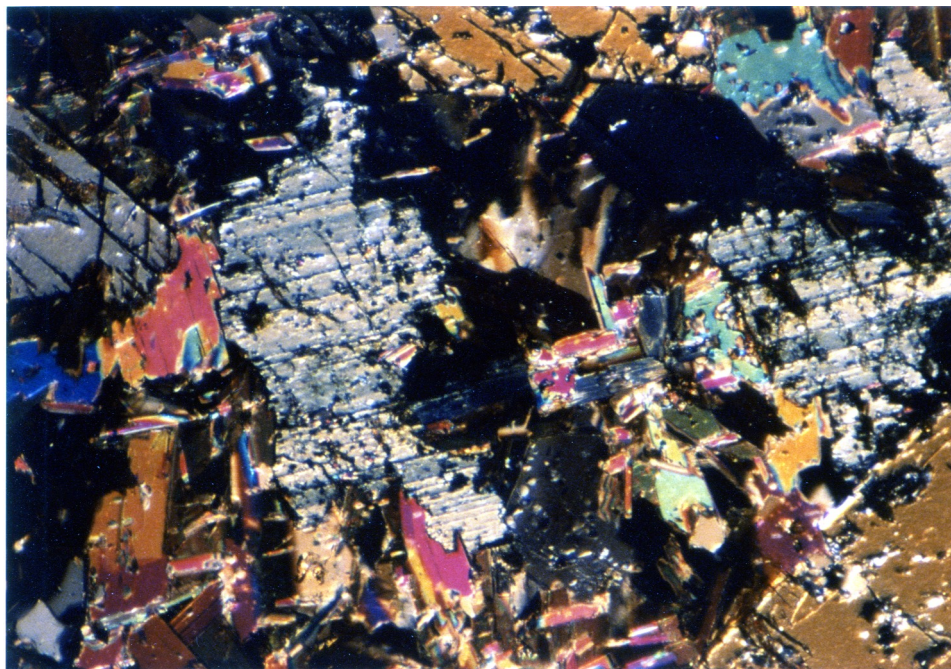


Figure 3-23. Photomicrograph of chloritoid that appears to be unstable from PM32b (long direction is ~3 mm).

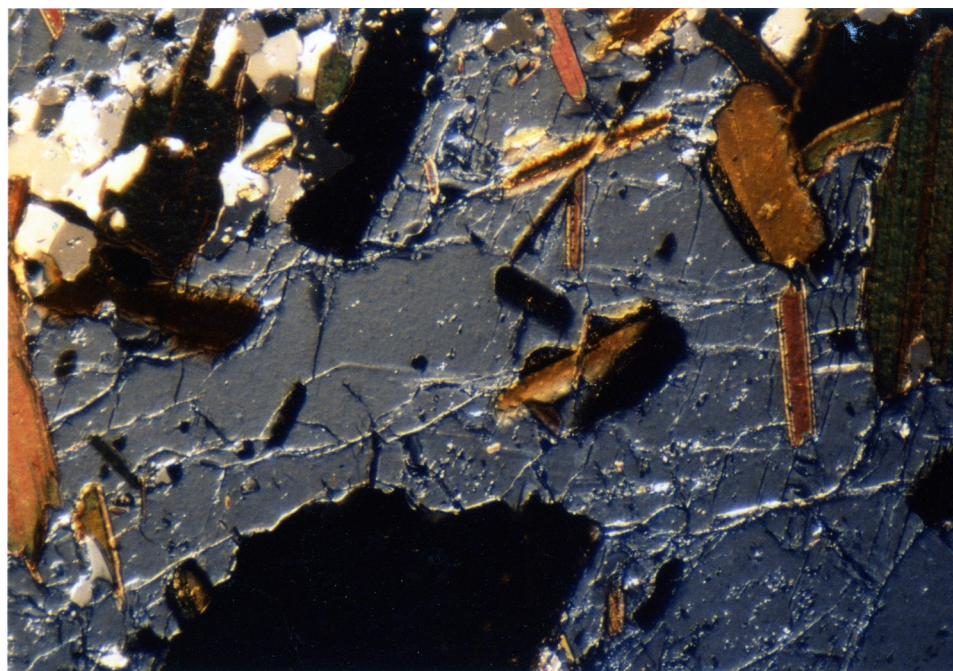


Figure 3-24. Photomicrograph of sample PM32b showing late andalusite with inclusions of biotite (long direction is ~5 mm).





Figure 3-25. Photomicrograph of garnet made up of numerous small garnets from PM32b (long direction is ~3 mm).

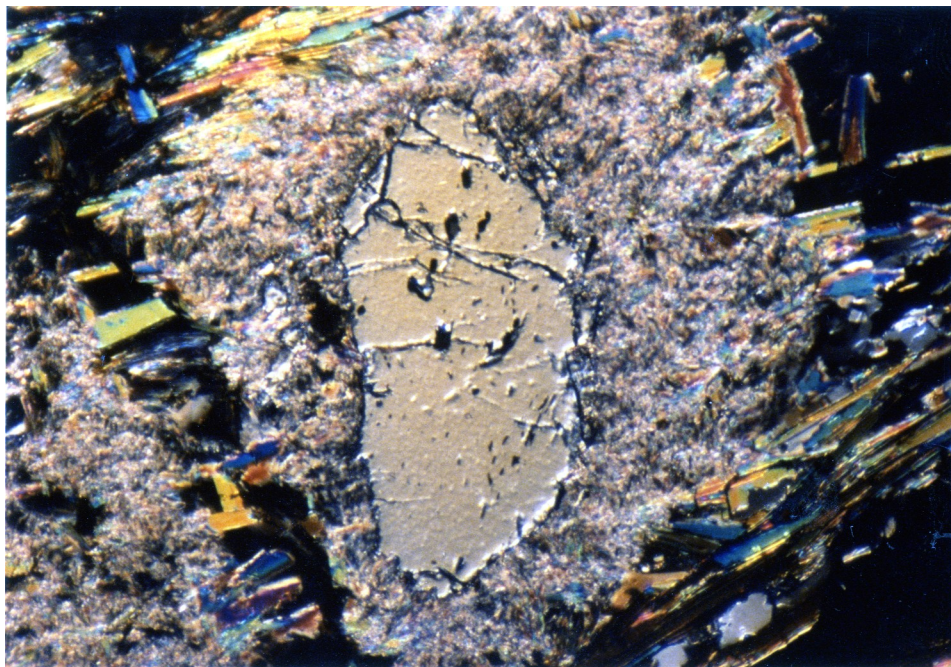


Figure 3-26. Photomicrograph of resorbed staurolite rimmed by muscovite in PM331 (long direction is ~3 mm).

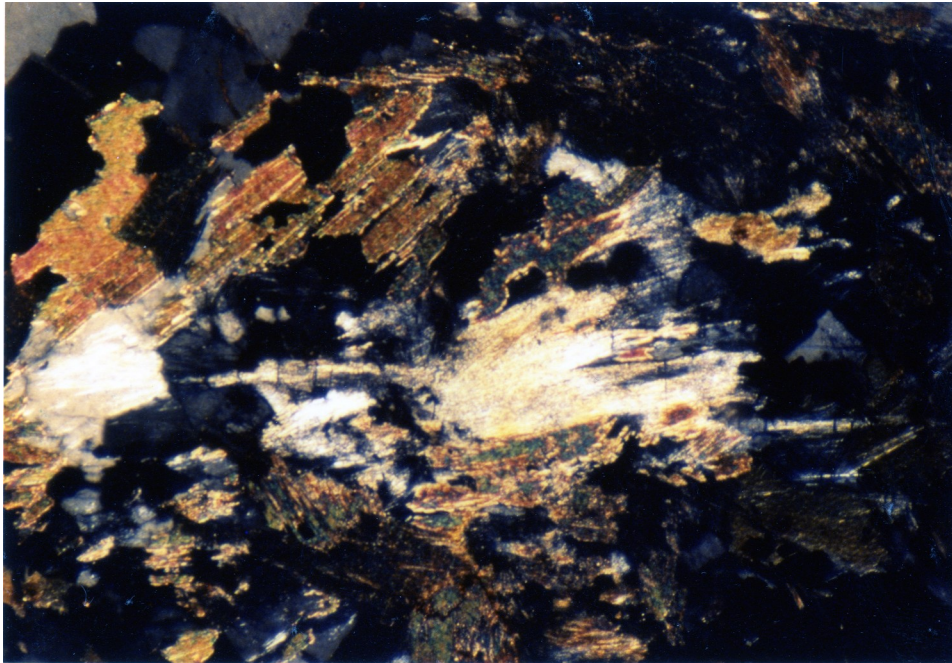


Figure 3-27. Photomicrograph of PM328 showing fibrolite (long direction is ~5 mm).



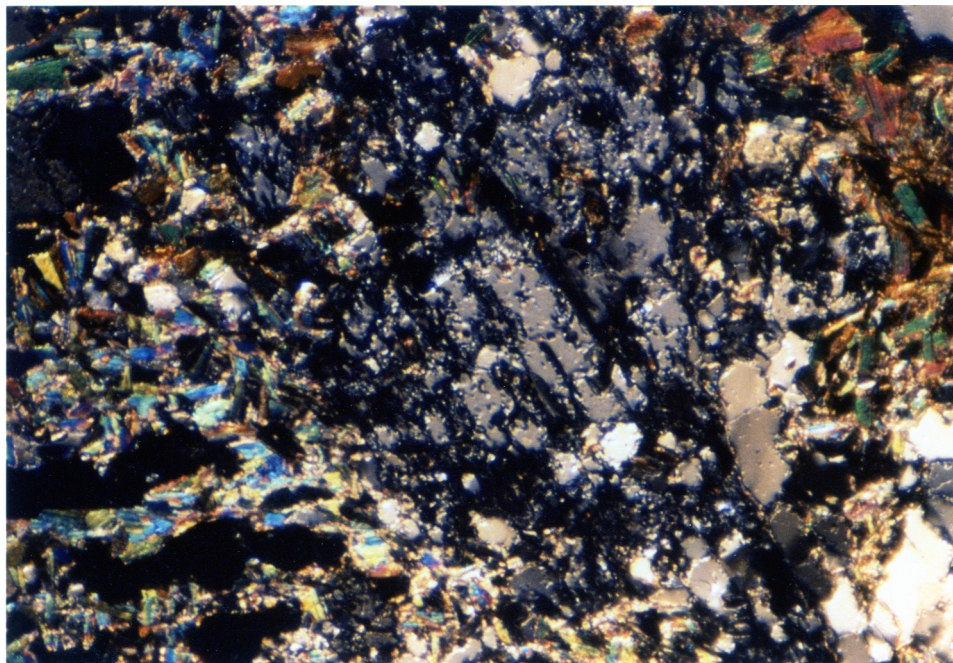


Figure 3-29. Photomicrograph showing resorbed kyanite in M1112 (long direction is ~3 mm).



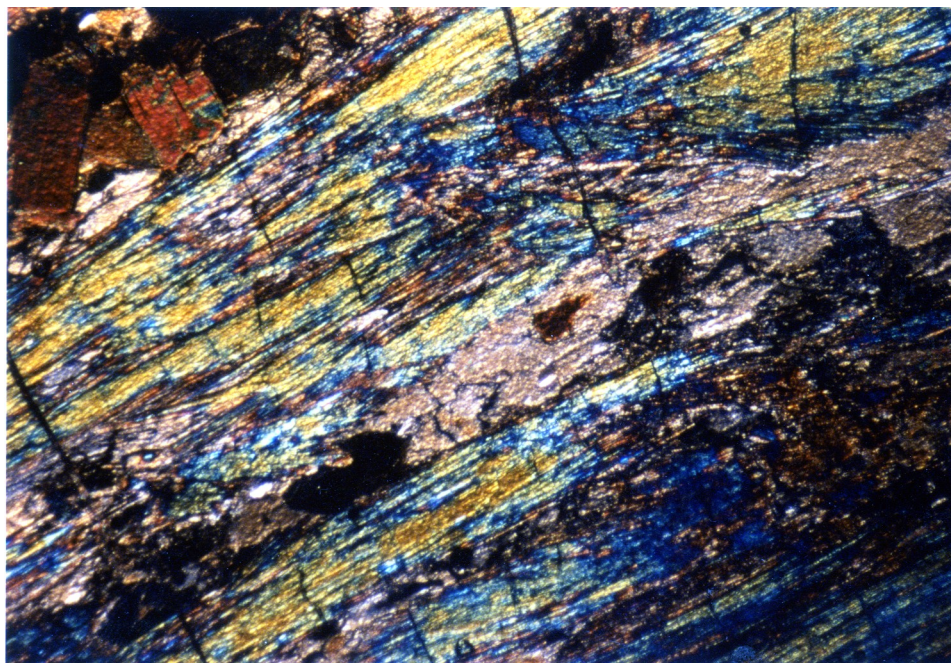


Figure 3-30. Photomicrograph of prismatic sillimanite and fibrolite from SG81 (long direction is ~5 mm).

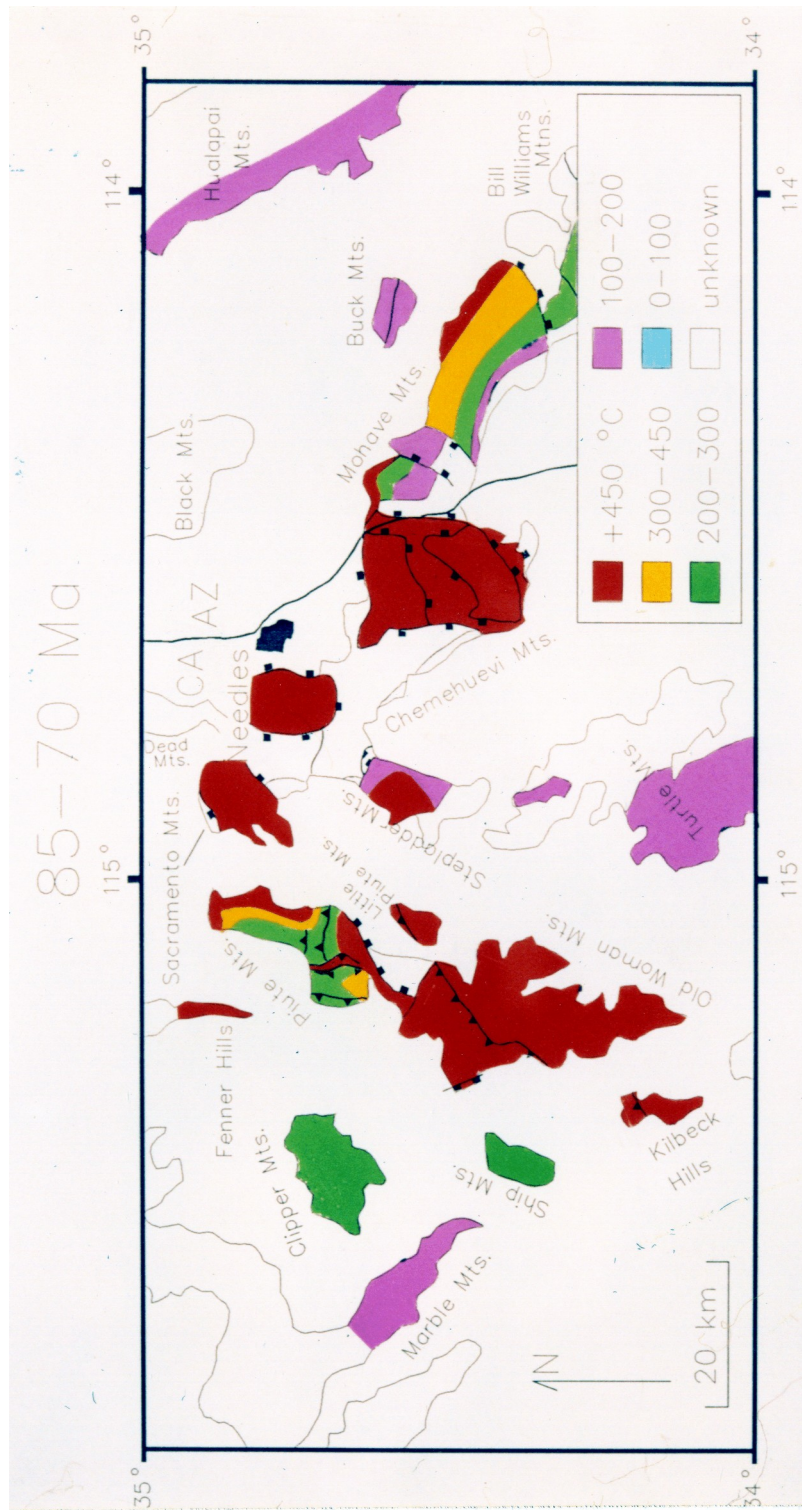


Figure 4-16. The apparent temperature distribution throughout the study area during the time interval 85-70 Ma. The temperatures are estimated from the  $^{40}\text{Ar}/^{39}\text{Ar}$  cooling ages of minerals and projected cooling rates calculated from suites of coexisting minerals.



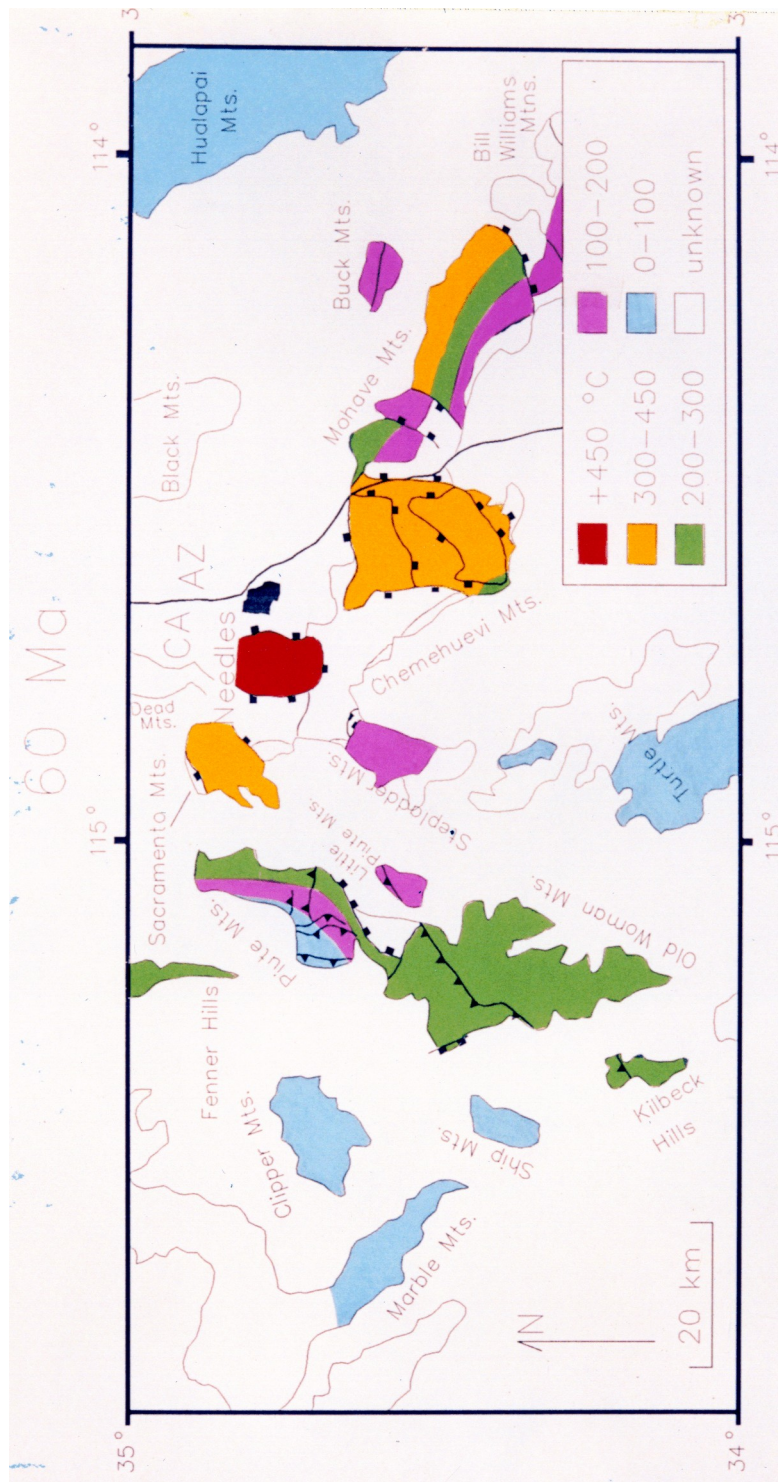


Figure 4-17. The apparent temperature distribution throughout the study area at 60 Ma. The temperatures are estimated from the  $^{40}\text{Ar}/^{39}\text{Ar}$  cooling ages of minerals and projected cooling rates calculated from suites of coexisting minerals.



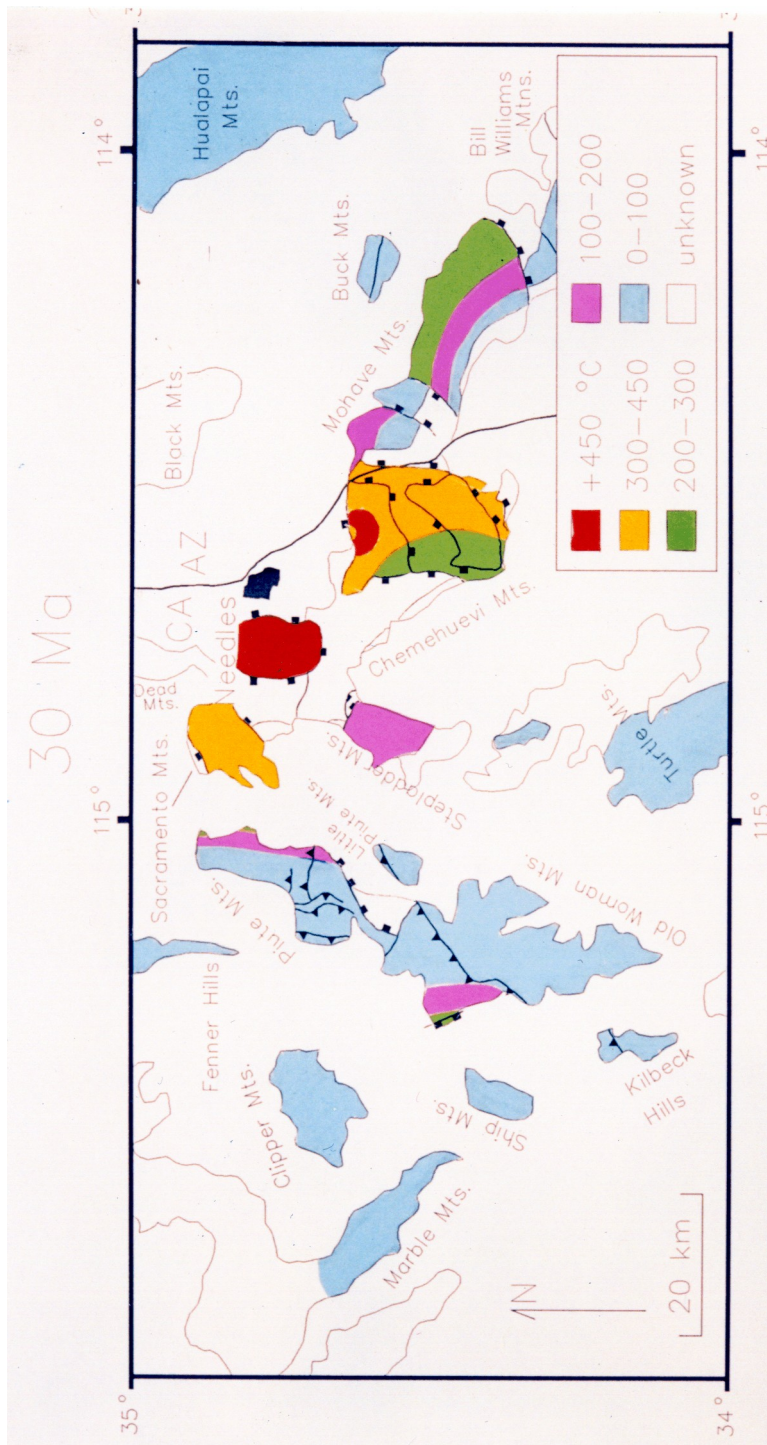


Figure 4-18. The apparent temperature distribution throughout the study area at 30 Ma. The temperatures are estimated from the  $^{40}\text{Ar}/^{39}\text{Ar}$  cooling ages of minerals and projected cooling rates calculated from suites of coexisting minerals.

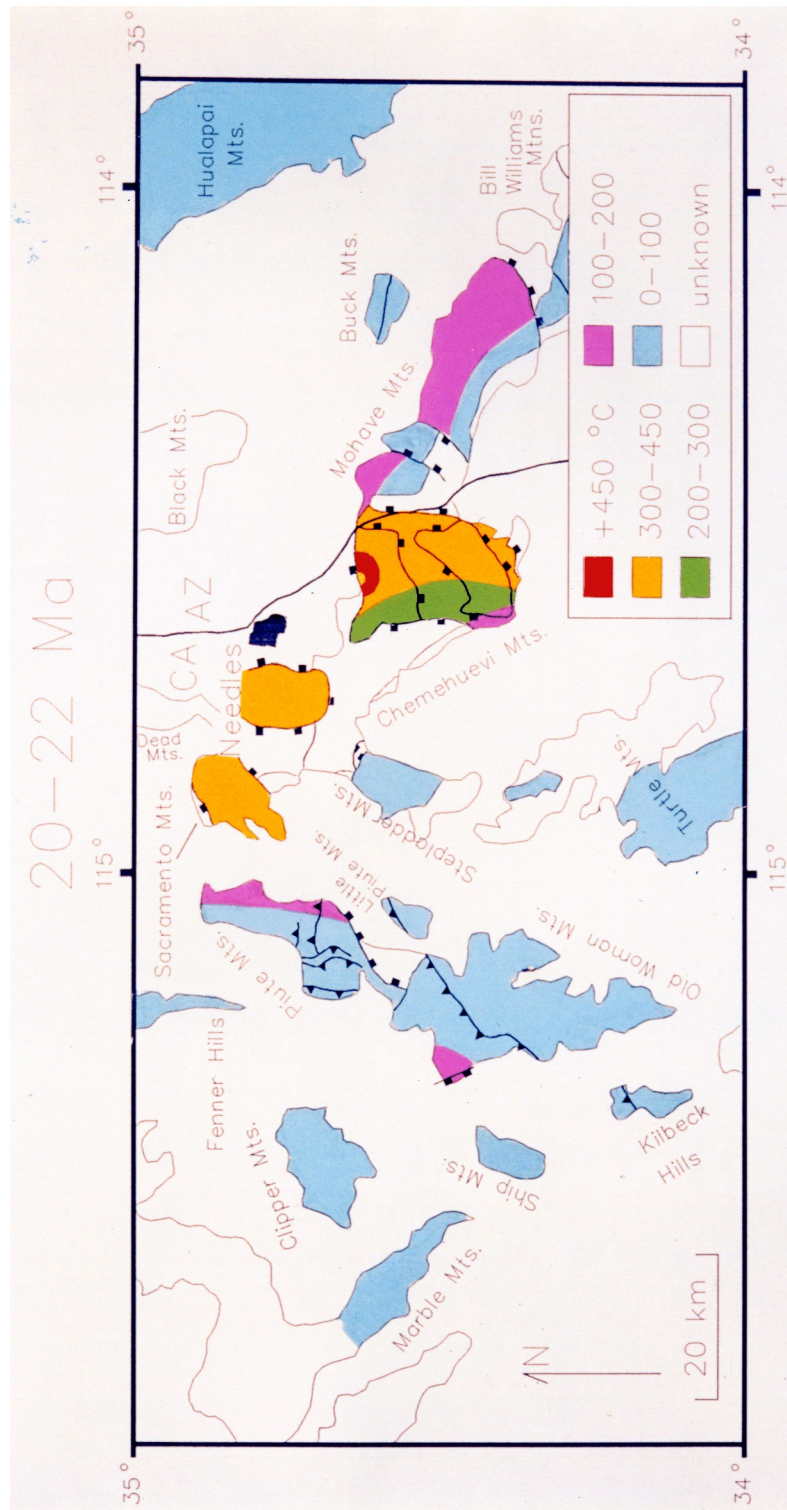


Figure 4-19. The apparent temperature distribution throughout the study area at 20 to 22 Ma. The temperatures are estimated from the  $^{40}\text{Ar}/^{39}\text{Ar}$  cooling ages of minerals and projected cooling rates calculated from suites of coexisting minerals.